13 Excretion Systems

KAZUYA MAEDA and YUICHI SUGIYAMA
Department of Molecular Pharmacokinetics, Graduate School of Pharmaceutical Sciences, The University of Tokyo, Bunkyo-ku, Tokyo, Japan

In previous chapters, the expression and function of metabolic enzymes and drug transporters have been overviewed as important factors dominating ADME (the absorption, disposition, metabolism, and excretion) of drugs. As common features, each metabolic enzyme and transporter consists of a wide variety of isoforms, and the substrate specificity of each isoform is very broad, thereby providing an evolutionary ability to protect the body against numerous kinds of xenobiotics. Thus, a single compound can often be recognized by multiple metabolic enzymes and transporters as a substrate because it partly overlaps with different isoforms of enzymes and transporters. These molecules are appropriately located at several tissues in the body and increase efficiency in the detoxification of xenobiotics. For example, in the liver, efficient detoxification can be achieved by the sequential processing of compounds, such as in the cellular uptake from the blood circulation to hepatocytes via influx transporters, phase I and II metabolism, and biliary excretion via efflux transporters.

In this chapter, we present an overview of how combinations of enzymes and transporters work concertedly as a detoxification "system". Moreover, when evaluating the efficiency of detoxification quantitatively, because these molecules have different roles and do not function in parallel in this system, clearance of xenobiotics in each tissue cannot be expressed simply as the sum or product of an intrinsic clearance of each isoform of metabolic enzymes and transporters. Therefore, we will also discuss theoretical considerations and experimental methods to evaluate the influence of the function of each molecule on the overall efficiency of a detoxification system from the viewpoint of pharmacokinetics.

Encyclopedia of Drug Metabolism and Interactions, 6-Volume Set, First Edition.
Edited by Alexander V. Lyubimov.

13.1 VECTORIAL TRANSPORT OF XENOBIOTICS IN TISSUES

Most xenobiotics are transferred to the liver and kidney, extensively metabolized in the liver, and excreted into bile and urine as an unchanged form or as metabolites for detoxification. In those processes, compounds must pass through both the basal and the apical membranes of hepatocytes and kidney tubular epithelial cells to reach the bile and urine compartments: this is called *transcellular transport* [1]. Such transcellular transport of drugs can also be seen in various other tissues such as intestinal epithelial cells as a site of drug absorption and the brain capillary endothelial cells as a major component of the blood–brain barrier. In general, because gap junctions seal the intercellular space tightly and transport between cells is very limited, transcellular transport is a major contributor to drug movement across cells, although paracellular transport sometimes plays a partial role in the intestinal absorption of small hydrophilic compounds according to Renkin's equation [2]. To enhance the efficiency of detoxification, basal-to-apical directional transcellular transport ("vectorial transport") of compounds is achieved with the aid of uptake and efflux transporters. For example, in the liver and kidney, several uptake transporters are expressed on the basal membrane facing the blood circulation and efflux transporters are expressed on the apical membrane facing the bile or urine. This allows the compounds to be concentrated into the bile and urine from the systemic blood.

For lipophilic compounds, because they can penetrate the plasma membrane easily, vectorial transport can be achieved only by the expression of efflux transporters. However, hydrophilic compounds cannot access efflux transporters because of their poor membrane permeability, and thus, both uptake and efflux transporters are required for their transcellular transport. For example, the bile-to-plasma concentration ratio of pravastatin, a nonmetabolized type of HMG-CoA reductase inhibitor (statin), is calculated to be about 960 in rats [3]. In fact, pravastatin is well known to be a substrate of the hepatic uptake transporter, OATP (organic anion transporting polypeptide) 1B1 and the efflux transporter, MRP2 (multidrug resistance-associated protein 2), which contribute to its concentrative transport in the bile and subsequent efficient excretion [4]. Such vectorial transport can be utilized in other tissues such as the small intestine and blood–brain barrier to strictly regulate the flux of necessary and unnecessary compounds in the body [1].

As shown in Fig. 13.1, vectorial transport is mediated by two different types of transporters, the ABC (ATP-binding cassette) family and the SLC (solute carrier) family transporters. The ABC family transporters are driven by the hydrolysis of intracellular ATP and mediate efflux transport from the inside to the outside of cells. Conversely, the SLC family transporters can transport compounds bidirectionally, depending on the concentration gradient of the driving force. For example, hepatic OATP family transporters generally take up compounds from the blood to hepatocytes, although the endogenous driving force has not been fully clarified [5], whereas the apically localized renal MATE (multidrug and toxin extrusion) transporters are considered to be involved in the efflux of cationic drugs into the urine driven by an exchange of H^+ ions [6]. The combinations of transporters for the transcellular transport of compounds differ depending on the physicochemical properties of compounds. In the case of organic anions, because the intracellular compartment is negatively charged and it is difficult for anions to gain access to the inside of cells from the outside via facilitated diffusion, active transport machineries must be involved in their uptake. Their efflux involves

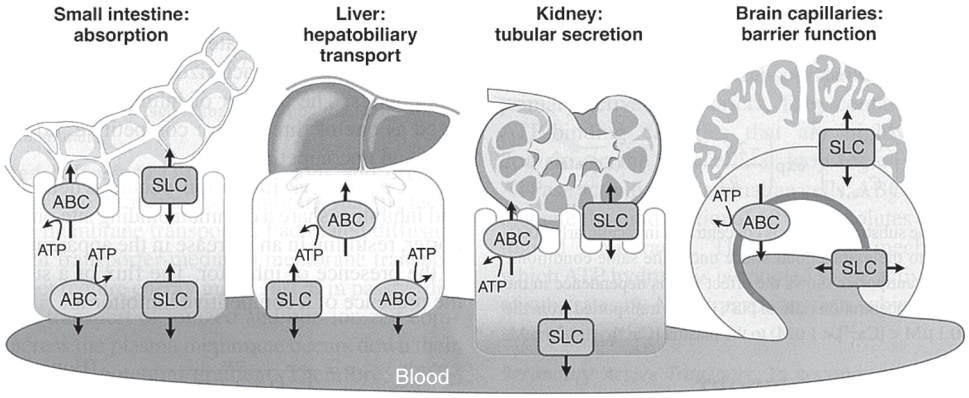

Figure 13.1 Role of SLC and ABC transporters in the transcellular transport of compounds in various tissues. Key: ABC, ATP-binding cassette transporter; SLC, solute carrier-type transporter. *Source*: This figure is cited from Ref. 1.

both facilitated diffusion-type transporters, such as OSTα/β (organic solute transporter α/β), and ABC transporters, such as MDR1 (multidrug resistance 1) and MRP2. On the other hand, in the case of cationic compounds, their uptake is mediated by facilitated diffusion-type transporters such as OCTs (organic cation transporters), whereas active transport mechanisms such as MATEs are mainly involved in their efflux.

Table 13.1 shows some examples of vectorial transport of endogenous and exogenous compounds mediated by the cooperation of uptake and efflux transporters [7]. Bile acids are distributed predominantly in the gastrointestinal tract and liver. This is achieved by the efficient enterohepatic circulation, consisting of both a transcellular transport system in the liver mediated by NTCP (Na^+-taurocholate cotransporting polypeptide) and BSEP (bile salt export pump), and in the intestine mediated by ASBT (apical Na^+-dependent bile acid transporter) and OSTα/β [8]. This type of enterohepatic circulation also benefits the pharmacological and toxicological effects of statins. For example, the transcellular transport of pravastatin in the liver is dominated by OATPs (uptake) and MRP2 (efflux), and its reuptake in the small intestine is thought to be mediated by the OATP family transporters [4]. The enterohepatic circulation contributes to the long-term accumulation of statins in the liver and to the subsequent sustained exposure to intrahepatic HMG-CoA reductase, a pharmacological target of statins. It also contributes to their low level in the blood circulation and a decreased risk of myopathy, which is one of the major side effects of statins.

TABLE 13.1 Transporter-Mediated Vectorial Transport of Compounds in the Tissues

Organ	Substrates	Basal Transporter	Direction	Apical Transporter
Liver	Organic anions	OATP1B1/OATP1B3/ OATP2B1	→	MDR1/MRP2/BCRP
	Bile acids	NTCP	→	BSEP
Kidney/small intestine	Dipeptide/peptide mimetics	(not identified)	←	PEPT1/PEPT2
Kidney	Organic anions	OAT1/OAT3	→	RST/NPT1/NPT4/ MRP4/MRP2/ OAT4/BCRP/ MDR1
	Organic cations	OCT2	→	OCTN1/OCTN2/ MATE1/MATE2/ MDR1
	Glucose	GLUT1/GLUT2	←	SGLT
	Nucleobase	ENT	←	CNT
	Carnitine	(not identified)	←	OCTN2
	Urate	OAT1/OAT3	→	NPT4
	Urate	GLUT9	←	RST
Intestine	Bile acids	OSTa/b	←	ASBT
	Folate/folate analogs	(not identified)	←	PCFT/RFC

Direction: →, basal-to-apical transport, ←, apical-to-basal transport.
Please note that combinations of transporters involved in the vectorial transport largely depends on the compounds.
This table contains some transporters whose *in vivo* role in the vectorial transport of compounds has not been fully clarified.
Source: This table is cited from Ref. 7 with some modifications.

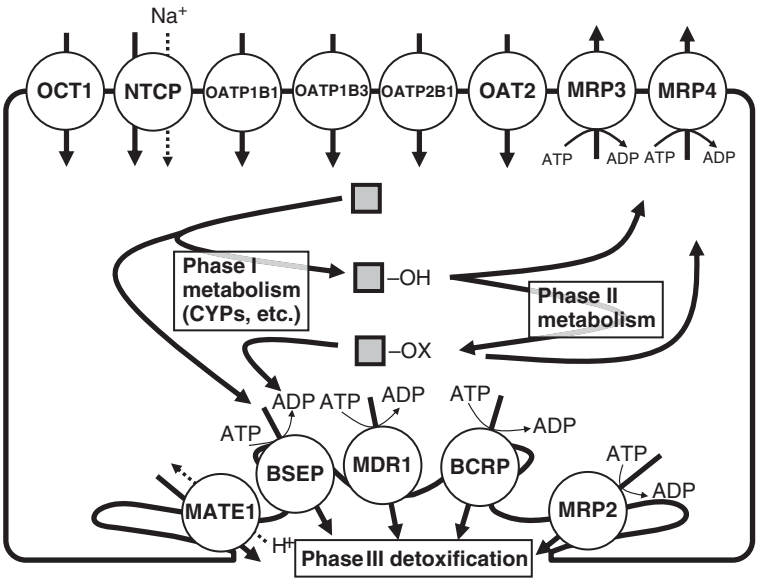

Figure 13.2 Major systems of drug detoxification in hepatocytes.

13.1.1 Vectorial Transport Machineries in the Liver

Figure 13.2 illustrates the major transporters expressed in hepatocytes. As mentioned above, transcellular transport of bile acids is mainly dominated by NTCP and BSEP. Clinically important anionic drugs including statins and angiotensin II receptor antagonists (sartans) are taken up into hepatocytes mainly via OATP1B1 and OATP1B3. Because the substrate specificities of OATP1B1 and OATP1B3 are very broad and are similar to each other, one compound is often recognized by both transporters. Previous reports suggested that the relative contribution of OATP1B1 and OATP1B3 to the hepatic uptake differs between substrates, although these anionic compounds accumulate preferentially in the liver [9]. For example, the hepatic uptake of valsartan is mediated by both OATP1B1 and OATP1B3 to the same extent [10], but that of telmisartan is exclusively dominated by OATP1B3 [11] even in the same category of drugs (sartans). These differences in the contribution of each transporter affect the extent of change in the overall intrinsic clearance of these compounds when the function of a single transporter is altered by genetic polymorphisms or drug interactions. OAT2 is also expressed on the basal membrane in the hepatocytes and accepts various structurally unrelated compounds such as bumetanide, zidovudine, 5-fluorouracil (5-FU), paclitaxel, and prostaglandin E_2 [12]. However, the relative contribution of OAT2 to the overall *in vivo* hepatic uptake of substrates is not fully understood.

OCT1 mediates hydrophilic organic cations with a relatively low molecular weight such as metformin and TEA (tetraethylammonium) [13]. Various kinds of ABC transporters expressed on the apical membrane are involved in biliary excretion. Generally, MDR1 preferentially transports various kinds of bulky hydrophobic and cationic compounds, MRP2 mainly transports anionic compounds including several conjugated metabolites such as glucuronide and glutathione conjugates, and BCRP can also

transport a wide variety of compounds, especially sulfated conjugates [14]. However, this rule is not always applicable to some compounds. MDR1 can sometimes transport anionic and zwitterionic drugs such as $E_2$17βG (estradiol-17β-glucuronide) and fexofenadine, and BCRP can transport cationic (cimetidine), zwitterionic (mitoxantrone), and neutral (topotecan) compounds as well as anionic compounds. Recent reports have shown that MATE1 is also expressed on the apical membrane of hepatocytes and is involved in the biliary excretion of cationic drugs such as metformin, since coadministration of pyrimethamine, a potent and specific inhibitor for MATEs, or gene knockout of MATE1 expression increased the hepatic distribution of metformin [15,16].

The vectorial transport of compounds mediated by uptake and efflux transporters in the liver was mimicked experimentally by the use of double-transfected cells. Originally, Cui *et al*. and Sasaki *et al*. constructed OATP1B3/MRP2 and OATP1B1/MRP2 double-transfected MDCKII cells, respectively, and they demonstrated the basal-to-apical vectorial transport of several organic anions in the monolayer of these cell systems on a transwell membrane insert [17,18]. Sasaki *et al*. have demonstrated that *in vivo* biliary clearance was predicted quantitatively from the vectorial transcellular transport of several compounds in rat Oatp1b2/Mrp2 double-transfected cells [19]. Subsequently, a set of double-transfected cells expressing OATP1B1/OATP1B3 (uptake) and MDR1/MRP2/BCRP (efflux) were constructed for rapid screening of the machineries involved in the vectorial transport of compounds [20]. For example, basal-to-apical vectorial transport of $E_2$17βG and pravastatin was largely enhanced in OATP1B1/MRP2 double-transfected cells compared with OATP1B1/MDR1 and OATP1B1/BCRP cells (Fig. 13.3), suggesting that the combination of OATP1B1-mediated uptake and MRP2-mediated efflux controls the efficient biliary excretion of these compounds [20]. This is supported by the drastic decrease in the biliary excretion of these compounds in the Mrp2-hereditary-deficient rat strain, EHBR (Eisai hyperbilirubinemic rat) [21,22]. Kopplow *et al*. have also constructed a quadruple-transfected cell line expressing OATP1B1, OATP1B3, OATP2B1, and MRP2 to better understand the substrate selectivity of MRP2 [23], because most of the substrates for that OATP family transporters are also substrates for MRP2, although they do not share homology with each other. For organic cations, double-transfected MDCKII cells expressing OCT1 and MDR1 were constructed and vectorial transport of berberine, a cationic plant alkaloid, was confirmed in this system [24]. Sato *et al*. have constructed OCT1/MATE1 double-transfected MDCK cells, and several cations such as TEA, metformin, and cimetidine could be transported vectorially from the basal to the apical sides of cell monolayers [25,26].

13.1.2 Vectorial Transport Machineries in the Kidney

Figure 13.4 illustrates the major transporters expressed in the proximal tubular epithelial kidney cells. OAT1 and 3 are thought to be involved mainly in the uptake of organic anions [12,27]. OAT1 accepts several kinds of small and hydrophilic organic anions such as PAH (*p*-aminohippurate) and nucleotide analog reverse-transcriptase inhibitors (adefovir, tenofovir, and cidofovir). On the other hand, OAT3 accepts a wide variety of bulky hydrophobic/amphipathic organic anions and its substrate specificity generally overlaps that of the OATP family transporters, although the protein sequences of these transporters are not similar. OAT3 can also transport cationic drugs such as histamine

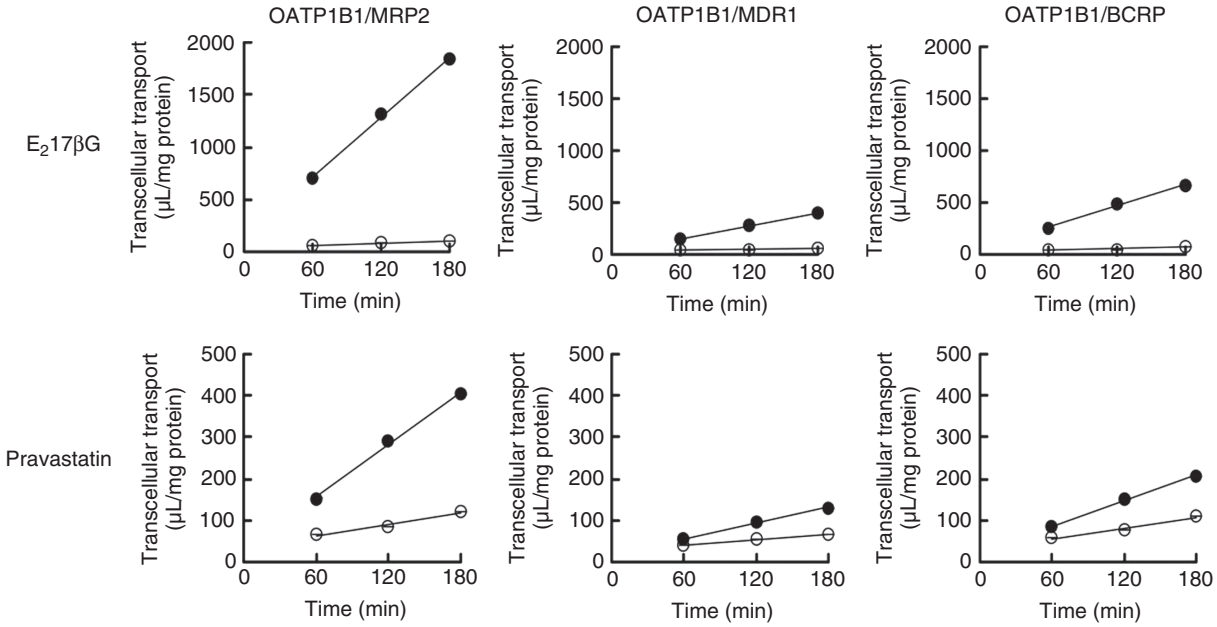

Figure 13.3 Transcellular transport of estradiol-17β-glucuronide ($E_2$17βG) and pravastatin in double-transfected cells expressing OATP1B1 and MDR1, MRP2, or BCRP. *Source*: This figure is cited from Ref. 20.

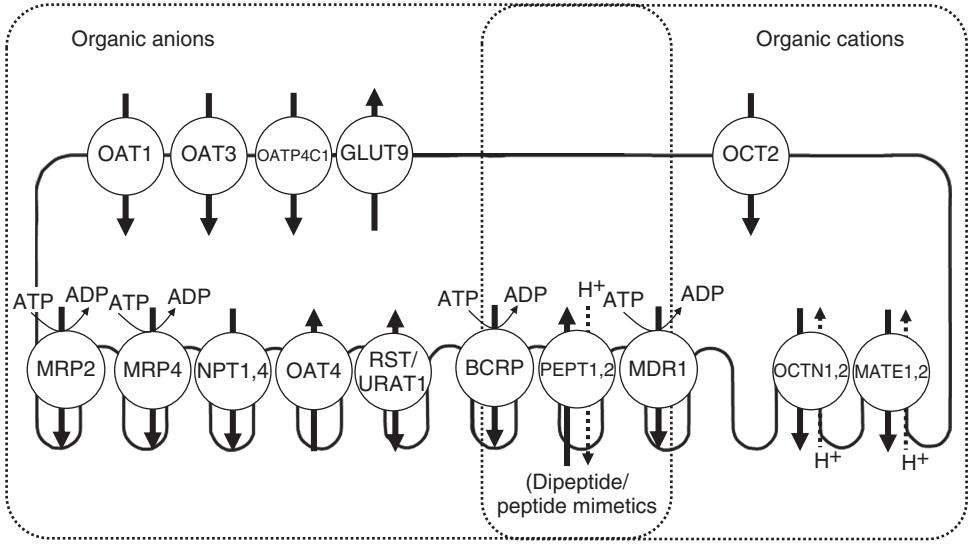

Figure 13.4 Major drug transporters for the transcellular transport of compounds in the kidney.

H_2 blockers (cimetidine, famotidine, ranitidine). As for the luminal efflux of intracellular anionic compounds to urine, considering the inside negative electrical potential, facilitated diffusion as well as active transport can be involved in the efflux of anionic compounds in the kidney. On the apical membrane, both ABC transporters such as MDR1, MRP2, MRP4, and BCRP and facilitative diffusion-type transporters such as RST [renal-specific transporter (in rodents); URAT1 (urate transporter) (in humans)], NPT (Na^+-dependent phosphate transport protein) 1, and NPT4 are known to be expressed [27]. Previous *in vitro* experiments using BBMVs (brush border membrane vesicles) suggested that at least two different transport systems, electroneutral exchange of organic anions and voltage-dependent facilitated diffusion, are involved in the luminal efflux of anions. However, there are few lines of evidence showing the importance of these transporters in the renal efflux of anions *in vivo*. The use of transporter knockout mice revealed that Bcrp is responsible for the luminal efflux of methotrexate, E3040 sulfate, and edaravone sulfate [28,29] and Mrp4 is involved in the luminal efflux of diuretics (hydrochlorothiazide and furosemide), antiviral drugs (adefovir and tenofovir), cephalosporins (ceftizoxime and cefazolin), and edaravone glucuronide [27]. In *in vitro* experiments using OAT3/RST double-transfected cells, basal to apical vectorial transport of benzylpenicillin, urate, and 2,4-dichlorophenoxyacetate was observed clearly, suggesting the role of these transporters in the urinary excretion of these compounds, although the significance of RST (URAT1) *in vivo* has not been demonstrated directly [30]. Urate is both secreted and reabsorbed in the kidney, and 90% of urate excreted via glomerular filtration is ultimately returned to the body. Recent clinical genetic studies and *in vitro* experiments suggested that the renal secretion of urate is thought to be dominated by uptake via OAT1/OAT3 and efflux via NPT4, while its reabsorption is mediated by uptake via URAT1 and efflux via GLUT (glucose transporter) 9 [31]. This hypothesis is partly supported by previous *in vivo* phenotypic observations of transporter knockout mice, although the metabolic fate of urate is totally different in rodents and humans. *In vitro* studies showed that NPT1 can transport some other organic anions such as PAH, benzylpenicillin, faropenem, and $E_2$17βG and that NPT4 can transport PAH, estrone-3-sulfate, $E_2$17βG, bumetanide, and ochratoxin A [32,33]. Thus, these NPT transporters might also contribute to the secretory vectorial transport of anionic compounds in cooperation with OATs.

Conversely, the renal uptake of hydrophilic and small organic cations is mainly mediated by OCT2 [34]. OCTN1, OCTN2, and MATEs, as well as MDR1 are expressed on the apical side of renal tubular epithelial cells. However, the transporter responsible for the renal efflux of cationic compounds *in vivo* is still under investigation, as it presumably acts in cooperation with OCT2. Ohashi *et al*. demonstrated that the renal secretion clearance of TEA was reduced to half in OCTN2-deficient *jvs* (juvenile visceral steatosis) mice, suggesting the importance of OCTN2 in the efflux of TEA in the kidney [35]. MATE family transporters (MATE1, MATE2, and MATE2-K) accept various kinds of organic cations such as metformin, fexofenadine, antiviral drugs (acyclovir, ganciclovir), anticancer drugs (oxaliplatin, cisplatin, and topotecan), and antibiotics (cephalexin, cephradine, and levofloxacin) [36,37]. Recent studies *in vivo* indicated that the kidney-to-plasma concentration ratios of TEA and metformin were increased by the coadministration of pyrimethamine, a potent selective MATE inhibitor, in mice. Moreover, the renal clearance of metformin, cephalexin, and cisplatin was decreased significantly in MATE1 gene knockout mice [15,16]. Kusuhara *et al*. also demonstrated that the renal clearance of metformin was decreased by 35%

when it was coadministered with pyrimethamine in healthy human subjects [38]. Thus, MATEs as well as OCT2 are considered to be responsible for the efficient secretory transport of metformin in the human kidney. *In vitro* experiments using OCT2/MATE1 double-transfected MDCK cells showed that the basal-to-apical transcellular transport of several cations such as TEA, metformin, cimetidine, procainamide, and quinidine was significantly higher than that in the opposite direction [25,26]. Thus, renal secretion of these compounds is thought to be dominated by uptake via OCT2 and efflux via MATE1.

As for reabsorption process in the kidney, although it is well known that several nutrients (e.g., amino acids, sugars, and vitamins) extensively undergo renal reabsorption from the lumen side, the combinations of uptake and efflux transporters dominating apical-to-basal vectorial transport of xenobiotics have not yet been fully clarified. Knockout of PEPT2, a peptide transporter, increased the renal clearance of cephadroxil and carnosine, suggesting that PEPT2 is involved in their renal reabsorption [39]. However, the transporters responsible for the basal efflux have not been determined. Oatp1a1 is also expressed on the apical renal membrane in male rats but almost not in female rats [40,41]. Previous studies demonstrated that the renal clearance of $E_2$17βG, dibromosulfophthalein, and zenarestat was significantly higher in male than in female rats, suggesting a role for Oatp1a1 in the uptake of compounds at the apical side of the kidney [40,41]. In contrast, there is no information about the corresponding OATP transporter gene expressed on the apical membrane of human kidneys or about the gender differences in the renal clearance of compounds in humans.

13.2 KINETIC CONSIDERATION OF KEY FACTORS DETERMINING THE ORGAN CLEARANCE

Excretion systems in the liver and kidney consist of multiple uptake and efflux transporters and metabolic enzymes. Because these molecules do not work sequentially one by one or in parallel for the detoxification of xenobiotics, organ clearance, an indicator for the performance of the detoxification system, cannot be simply defined by the sum or product of the intrinsic activity (transport/metabolism) of each molecule. In each process such as uptake, efflux, and metabolism, multiple molecules are involved simultaneously, thanks to their broad and overlapping substrate specificities. Thus, we must consider the relative contribution of each molecule to the overall activity of each step. Organ intrinsic clearance is dominated by uptake, efflux, backflux to the blood circulation, and metabolism and can be described theoretically by using the intrinsic activity of each step. Then, organ clearance can be estimated from multiple factors such as the overall intrinsic clearance, blood flow, and protein unbound fraction in a model-dependent manner. In this section, we describe how the intrinsic activity of each molecule affects the performance of detoxification system in the *in vivo* situation quantitatively, from the viewpoint of pharmacokinetic theory. Such a consideration is essential to estimate the extent of change in the total clearance and exposure of drugs in the body when the expression and function of each molecule are altered by several factors such as genetic polymorphisms, interacting drugs, and pathophysiological conditions.

13.2.1 Contribution of Each Isoform to the Overall Metabolism/Transport

In each step of detoxification such as uptake, efflux, backflux, and metabolism, multiple transporters or metabolic enzymes often work in parallel. For metabolism, metabolic intrinsic clearance (CL_{met}) can be simply described as the sum of the intrinsic clearance of each metabolic enzyme ($CL_{enzyme,i}$) as

$$CL_{met} = CL_{enzyme,1} + CL_{enzyme,2} + \cdots + CL_{enzyme,i} \tag{13.1}$$

On the other hand, for the membrane transport of lipophilic compounds, we must also think about the contribution of passive permeation as well as active transport. Thus, intrinsic membrane transport clearance ($PS_{transport}$) is the sum of the intrinsic clearance of passive transport ($CL_{passive}$) and active transport mediated by each transporter ($CL_{TP,i}$).

$$PS_{transport} = CL_{passive} + CL_{TP,1} + CL_{TP,2} + \cdots + CL_{TP,i} \tag{13.2}$$

The impact of the relative contribution of each molecule on the overall intrinsic clearance can be tested virtually in a model case. Assuming that drug A is eliminated only by the hepatic metabolism and that its pharmacokinetics follow the well-stirred model, when drug A is orally administered, the area under the plasma concentration–time curve (AUC) can be described by the following equation.

$$\begin{aligned} AUC_{oral} &= \frac{F_a F_g \cdot F_h \cdot \text{Dose}}{CL_h} = \frac{F_a F_g \frac{Q_h}{Q_h + f_B CL_{int,h}} \text{Dose}}{\frac{Q_h f_B CL_{int,h}}{Q_h + f_B CL_{int,h}}} = \frac{F_a F_g \cdot \text{Dose}}{f_B CL_{int,h}} \\ &= \frac{F_a F_g \cdot \text{Dose}}{f_B \left(CL_{enzyme,1} + CL_{enzyme,2} + \cdots + CL_{enzyme,i}\right)} \end{aligned} \tag{13.3}$$

Here, $F_a F_g$ is the intestinal availability, F_h the hepatic availability, CL_h the hepatic clearance, Q_h the hepatic blood flow rate, f_B the protein unbound fraction in blood, and $CL_{int,h}$ the hepatic intrinsic clearance.

Under this situation, if the function of enzyme 1 is decreased to $1/R$, the fold increase in the AUC_{oral} value largely depends on the relative contribution of intrinsic clearance mediated by enzyme 1 to the overall metabolic clearance ($f_{m,1}$).

$$\begin{aligned} AUC_{oral}\ \text{ratio} &= \frac{f_B \left(CL_{enzyme,1} + CL_{enzyme,2} + \cdots + CL_{enzyme,i}\right)}{f_B \left(\frac{CL_{enzyme,1}}{R} + CL_{enzyme,2} + \cdots + CL_{enzyme,i}\right)} \\ &= \frac{f_{m,1} \cdot CL_{int,h} + (1 - f_{m,1}) CL_{int,h}}{f_{m,1} \cdot \frac{CL_{int,h}}{R} + (1 - f_{m,1}) CL_{int,h}} = \frac{1}{f_{m,1} \cdot \frac{1}{R} + (1 - f_{m,1})} \end{aligned} \tag{13.4}$$

Following Equation 13.4, the fold increase in the AUC_{oral} is plotted against the inhibition potency of enzyme 1 (R) in Fig. 13.5. If enzyme 1 is inhibited potently, the AUC_{oral} ratio shows large difference even when the relative contribution ($f_{m,1}$) changes slightly. Thus, the quantitative estimation of the contribution of each molecule to the overall intrinsic clearance is important if we correctly predict the AUC change caused by the functional change of a single molecule.

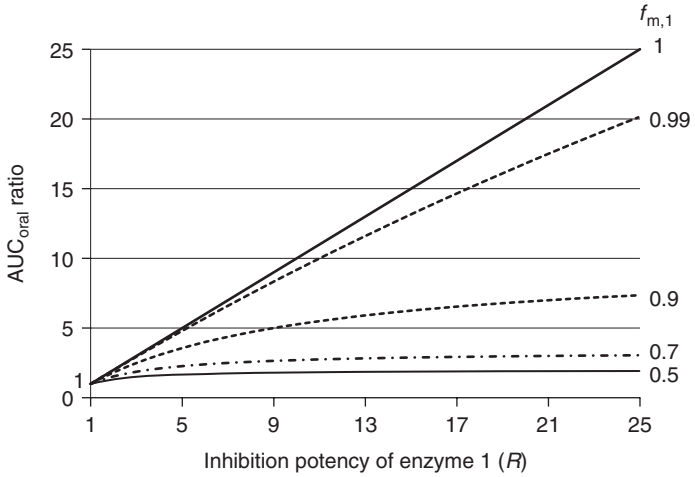

Figure 13.5 Importance of the contribution of a specific enzyme to the overall metabolism in the increase of the AUC_{oral} value. Theoretical calculation of the AUC_{oral} ratio (AUC_{oral} (+inhibitor)/AUC_{oral} (control)) is performed when enzyme 1 contributes $f_{m,1}$ values of 1.0, 0.99, 0.9, 0.7, and 0.5 of the total metabolic activity and the metabolic activity of enzyme 1 is specifically decreased to $1/R$.

Niemi *et al*. [42] showed that the AUC of repaglinide, a substrate of CYP2C8 and CYP3A4, was increased by 8.1-fold in coadministration with gemfibrozil, a potent inhibitor of CYP2C8, and increased by 1.4-fold in coadministration with itraconazole, a potent inhibitor of CYP3A4. On the other hand, in coadministration with both gemfibrozil and itraconazole, the AUC of repaglinide increased greatly by 19.4-fold [42]. This seems to be a synergistic inhibitory effect of gemfibrozil and itraconazole. However, this kind of drug interaction can be explained only by conventional pharmacokinetic theory, considering the contribution of each molecule. We assume that drug B is eliminated by three different metabolic pathways mediated by enzymes X, Y, and Z, and that the relative contributions (f_m) of enzymes X, Y, and Z to the overall metabolism of drug B are 0.5, 0.4, and 0.1, respectively. In this situation, when drug B is coadministered with a potent inhibitor of enzyme X, according to Equation 13.4, the AUC of drug B is expected to be increased by 2-fold, while its AUC is increased by 1.7-fold when coadministered with a potent inhibitor of enzyme Y. On the other hand, when both enzymes X and Y are completely inhibited by coadministration of both inhibitors, the AUC of drug B is increased drastically up to 10-fold because the metabolic intrinsic clearance becomes one-tenth of that in a control situation. Therefore, it must be noted that a combination of inhibitor drugs for different metabolic pathways can sometimes increase the exposure of the victim drug significantly, although the complete inhibition of a single metabolic pathway does not affect the drug concentration so much.

A similar story is also discussed in a recent paper by Kusuhara and Sugiyama [43] concerning the apparent synergistic effect of the P-gp and BCRP on the brain distribution of substrates. There is some evidence demonstrating that the double knockout of P-gp and Bcrp expression in mice produced remarkable increases in the concentration of some drugs in the brain, whereas single knockouts of P-gp or Bcrp showed only

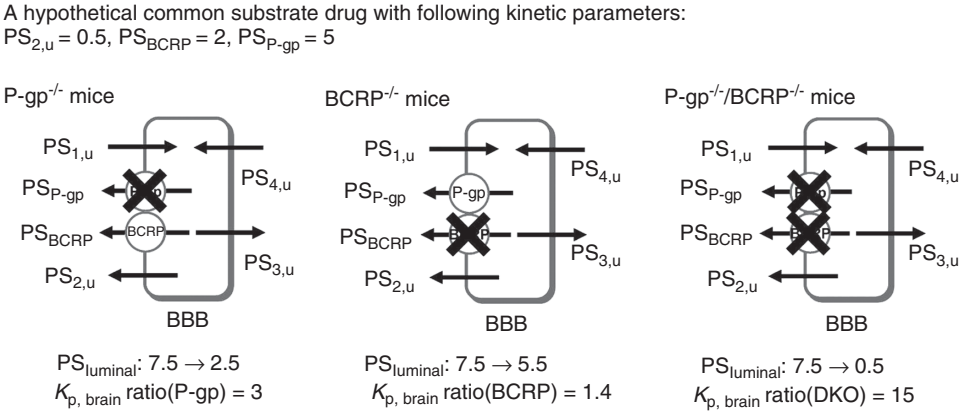

Figure 13.6 Theoretical consideration of the apparent synergistic effects of P-gp and BCRP knockout on the brain distribution of substrates. The simple model for the transcellular transport of compounds at the blood–brain barrier was constructed and $K_{p,brain}$ was estimated when each parameter was set at the designated values shown in this figure. Then, $K_{p,brain}$ values were compared between wild type, P-gp knockout, BCRP knockout, and P-gp/BCRP double-knockout mice. *Source*: This figure is cited from Ref. 43.

limited effects [44–46]. This apparent synergism can be explained by simple pharmacokinetic theory without considering any interplay between the P-gp and Bcrp [43,47]. Following the schematic diagram of the membrane transport in brain endothelial cells, brain-to-blood concentration ratio ($K_{p,brain}$) can be described by the parameters shown in Fig. 13.6 according to the following equation.

$$K_{p,brain} = \frac{PS_{blood\rightarrow brain}}{PS_{brain\rightarrow blood}} = \frac{PS_{1,u}\frac{PS_{3,u}}{PS_{P\text{-}gp}+PS_{BCRP}+PS_{2,u}+PS_{3,u}}}{PS_{4,u}\frac{PS_{P\text{-}gp}+PS_{BCRP}+PS_{2,u}}{PS_{P\text{-}gp}+PS_{BCRP}+PS_{2,u}+PS_{3,u}}}$$
$$= \frac{PS_{1,u}\cdot PS_{3,u}}{PS_{4,u}(PS_{P\text{-}gp}+PS_{BCRP}+PS_{2,u})} \quad (13.5)$$

Thus, the ratio of the $K_{p,brain}$ value in knockout mice to that in normal mice is

$$K_{p,brain}\ \text{ratio(P-gp)} = \frac{\frac{PS_{1,u}\cdot PS_{3,u}}{PS_{4,u}(PS_{BCRP}+PS_{2,u})}}{\frac{PS_{1,u}\cdot PS_{3,u}}{PS_{4,u}\cdot(PS_{P\text{-}gp}+PS_{BCRP}+PS_{2,u})}} = 1+\frac{PS_{P\text{-}gp}}{PS_{BCRP}+PS_{2,u}} \quad (13.6)$$

$$K_{p,brain}\ \text{ratio(BCRP)} = \frac{\frac{PS_{1,u}\cdot PS_{3,u}}{PS_{4,u}(PS_{P\text{-}gp}+PS_{2,u})}}{\frac{PS_{1,u}\cdot PS_{3,u}}{PS_{4,u}(PS_{P\text{-}gp}+PS_{BCRP}+PS_{2,u})}} = 1+\frac{PS_{BCRP}}{PS_{P\text{-}gp}+PS_{2,u}} \quad (13.7)$$

$$K_{p,brain}\ \text{ratio(P-gp/BCRP)} = \frac{\frac{PS_{1,u}\cdot PS_{3,u}}{PS_{4,u}\cdot PS_{2,u}}}{\frac{PS_{1,u}\cdot PS_{3,u}}{PS_{4,u}(PS_{P\text{-}gp}+PS_{BCRP}+PS_{2,u})}} = 1+\frac{PS_{P\text{-}gp}+PS_{BCRP}}{PS_{2,u}} \quad (13.8)$$

Therefore, when the absolute value of each parameter is set according to Fig. 13.6, the $K_{p,brain}$ ratios in P-gp and Bcrp single-knockout mice increase slightly by 3- and 1.4-fold, respectively, whereas that in P-gp/Bcrp double-knockout mice largely increases by 15-fold, which reproduces the apparent synergism of the *in vivo* observation [43].

Predictive methods to estimate the relative contribution of each molecule to the overall intrinsic clearance have been established and validated in the fields of both metabolic enzymes and transporters. For metabolism, Crespi and Penman [48] originally published the concept of the RAF (relative activity factor) method. In this, the metabolic clearance of a test compound and a selective substrate for each enzyme is measured in liver microsomes, and the recombinant enzyme expression system and the ratio of the clearance of each selective substrate in liver microsomes to that in the expression system are estimated for each enzyme ($R_{enzyme,i}$). Then, the contribution of enzyme 1 to the overall metabolic enzyme ($f_{m,enzyme,1}$) can be described as follows.

$$f_{m,enzyme,1} = \frac{R_{enzyme,1} \cdot CL_{test,enzyme,1}}{\sum_i R_{enzyme,i} \cdot CL_{test,enzyme,i}} \left(= \frac{R_{enzyme,1} \cdot CL_{test,enzyme,1}}{CL_{int,h}} \right) \quad (13.9)$$

Here, $CL_{test,enzyme,i}$ is the metabolic clearance of a test compound in a recombinant expression system for enzyme i.

Now, an *in vitro* selective substrate for each CYP isoform has been established almost completely. Another method is to use a selective inhibitor for each isoform. In the field of CYP enzymes, chemical selective inhibitor and functional neutralizing antibody for each major CYP isoform have also been established. The metabolic clearance of a test compound is measured in the absence and presence of a selective inhibitor and then the contribution of enzyme 1 to the overall metabolic enzyme ($f_{m,enzyme,1}$) can be described as follows.

$$f_{m,enzyme,1} = 1 - \frac{CL_{test}(+inhibitor)}{CL_{test}(-inhibitor)} \quad (13.10)$$

Similar methods can be used in the field of drug transporters. Kouzuki *et al*. [49,50] applied the RAF method to estimate the relative contributions of Ntcp and Oatp1a1 to the overall uptake of compounds in rat hepatocytes. $E_2$17βG and taurocholate were used as selective substrates for Oatp1a1 and Ntcp, respectively, although $E_2$17βG is no longer used as a reference compound for Oatp1a1. Hirano *et al*. [51] have established a method for estimating the relative contribution of OATP1B1 and OATP1B3 to the overall uptake of $E_2$17βG and pitavastatin in human hepatocytes by using estrone-3-sulfate (E-sul) and cholecystokinin octapeptide (CCK-8) as selective substrates for OATP1B1 and OATP1B3, respectively. They calculated the ratio of the uptake clearance of the reference compounds in human cryopreserved hepatocytes to that in the transporter expression systems ($R_{act,transporter}$). The uptake clearance of test compounds mediated by a specific transporter in hepatocytes can be calculated by multiplying the $R_{act,transporter}$ value by the uptake clearance of test compounds in the expression system ($CL_{test,transporter}$). If we can assume that test compounds are taken up into hepatocytes exclusively by OATP1B1 and OATP1B3 then the uptake clearance of test compounds in hepatocytes ($CL_{test,hep}$) should be described by the following equation.

$$CL_{test,hep} = R_{act,OATP1B1} \cdot CL_{test,OATP1B1} + R_{act,OATP1B3} \cdot CL_{test,OATP1B3} \quad (13.11)$$

Using this method, they demonstrated that both $E_2$17βG and pitavastatin were taken up into hepatocytes mainly via OATP1B1. The use of a selective inhibitor for each isoform is also available to estimate the contribution of OATP1B1 and OATP1B3 to the uptake of compounds in human hepatocytes [11]. Thus, E-sul can be used as a specific inhibitor for OATP1B1. The uptake of $E_2$17βG and pitavastatin in human hepatocytes was almost inhibited in the presence of an excess of E-sul, which further supports the major contribution of OATP1B1. Conversely, telmisartan uptake was observed only in OATP1B3-expressing cells but not in OATP1B1-expressing cells and the uptake of telmisartan in human hepatocytes was not inhibited by E-sul, suggesting that telmisartan is transported predominantly by OATP1B3 [11]. Figure 13.7 summarizes our findings of the contributions of OATP1B1 and OATP1B3 to the hepatic uptake of substrates. Even in the same category of drugs, the relative importance of OATP1B1 and OATP1B3 is different between valsartan (OATP1B1 = OATP1B3) and telmisartan (OATP1B3 ≫ OATP1B1). This kind of information is useful when considering the effect of genetic polymorphisms and drug interactions on the changes in pharmacokinetics of substrate drugs. Previous clinical pharmacogenetic studies indicated that the pharmacokinetics of some statins are clearly affected by SNPs (single nucleotide polymorphism) in OATP1B1 but not telmisartan [52,53].

A similar type of investigation was also performed by using rat and human kidney slices to estimate the contribution of OAT1 and OAT3 to the renal uptake of compounds. Hasegawa *et al*. [54,55] have established a RAF method for renal uptake by using PAH and pravastatin as selective substrates for rat Oat1 and Oat3, respectively, and demonstrated that renal uptake clearance predicted using the RAF method was similar to that observed in rat kidney slices in most cases. Using this method, the contributions of Oat1 and Oat3 to the renal uptake of several uremic toxins have been determined, and these results were further validated by observing the inhibitory effects of PAH (an OAT1-selective inhibitor), PCG, and pravastatin (an OAT3-selective inhibitor) on their uptake in rat kidney slices [56].

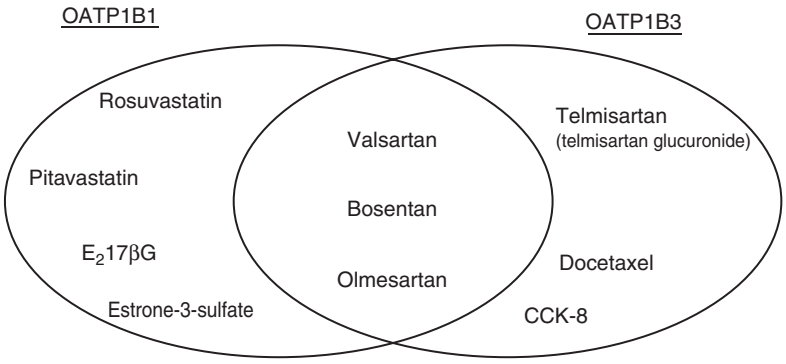

Figure 13.7 Relative contribution of OATP1B1 and OATP1B3 to the overall hepatic uptake of compounds estimated in human cryopreserved hepatocytes. This figure indicates which compounds are taken up in the hepatocytes, mainly mediated by OATP1B1 (left), OATP1B3 (right), or both OATP1B1 and OATP1B3 (center).

Sandwich-cultured hepatocytes have been utilized for the characterization of efflux from hepatocytes to the bile. LeCluyse *et al*. [57,58] have demonstrated that hepatocytes cultured between layers of collagen gel or Matrigel could efficiently repolarize and form what they termed a *bile pocket* between adjacent cells, which mimics the bile canalicular compartment in the liver and depletion of Ca^{2+} from the incubation medium rapidly disrupted the closed bile pocket by opening tight junctions. Thus, the amounts of compounds excreted into the bile pocket can be estimated by their differential cumulative uptake in sandwich-cultured hepatocytes preincubated with Ca^{2+}-containing and Ca^{2+}-free buffers. Recent studies succeeded in the use of siRNA for inhibiting each efflux transporter in determining its contribution to the overall efflux of compounds into the bile pocket. Tian *et al*. [59] demonstrated that knockdown of Mrp2 by siRNA in rat sandwich-cultured hepatocytes resulted in a 50% decrease in the protein expression and a 45% decrease in the biliary excretion index (BEI) of carboxydichlorofluorescein (CDF), which is reported to be excreted predominantly into the bile under the control of Mrp2 in rats. Bcrp knockdown by adenoviral vector-mediated RNAi (RNA interference) also succeeded, and the protein expression of Bcrp was drastically decreased to 5% of control at day 6 after starting the culture of rat hepatocytes, whereas the BEI value of nitrofurantoin, a selective substrate of Bcrp, was also decreased to 11% of control [60]. The BEI value of ^{99m}Tc-sestamibi, which is used for hepatobiliary scintigraphy, in the bile pocket was not decreased by treatment with a Bcrp siRNA-expressing adenovirus, but its efflux was totally abolished in the presence of GF120918, a typical inhibitor for both Mdr1 and Bcrp, suggesting that ^{99m}Tc-sestamibi can be used as a selective substrate for Mdr1 in rat hepatocytes [61].

Renal BBMVs are useful tools for characterizing efflux transport systems in the kidney [62]. However, because the responsible transporters have not been well characterized and the driving force of efflux transporters is required to be known for the transport assay using BBMVs, it is difficult to estimate the contribution of each transporter to the overall efflux of compounds in the kidney. For reabsorption, we can understand the involvement of reabsorption in the renal clearance qualitatively by observing the reduction in reabsorption by diuresis induced by mannitol [63]. However, there is no appropriate *in vitro* experimental system for the quantitative analysis of transporters involving reabsorption at present.

13.2.2 Rate-limiting Step of the Overall Intrinsic Clearance in a Tissue

In traditional pharmacokinetic theory, we normally regard the metabolic intrinsic clearance to be the same as the hepatic intrinsic clearance. Previous reports suggested that the *in vivo* hepatic clearance of various CYP substrate drugs could be well predicted from the *in vitro* metabolic intrinsic clearance estimated by using liver microsomes. However, this model cannot be applied to the transporter substrates, which are extensively excreted into bile as unchanged forms with minimal metabolism, such as some statins (pravastatin, pitavastatin, rosuvastatin) because the hepatic clearance is relatively large, while metabolic clearance is too low to be estimated. Lam *et al*. [64] suggested that the *in vivo* intrinsic clearance of digoxin could be better predicted from the *in vitro* intrinsic clearance with primary rat hepatocytes rather than that observed with liver microsomes. Frassetto *et al*. have also demonstrated in humans that the results of the erythromycin breath test, a typical clinical test to evaluate the CYP3A4 activity *in vivo*, were altered by coadministration of rifampicin, a typical

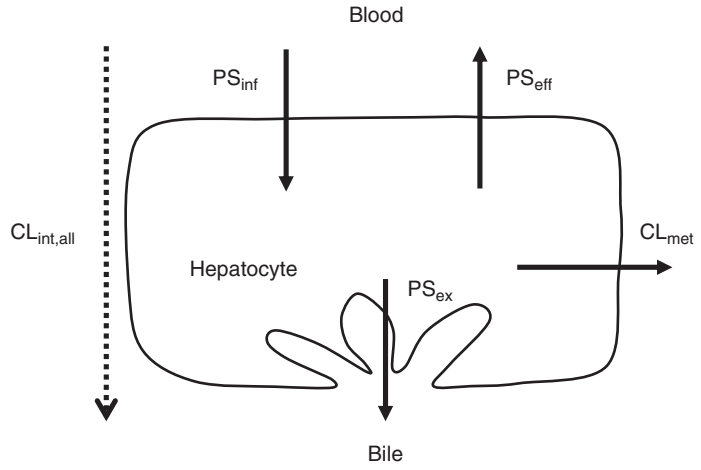

Figure 13.8 Scheme of hepatic transport and metabolism in hepatocytes for the theoretical consideration of overall hepatic intrinsic clearance ($CL_{int,all}$).

OATP inhibitor, and lansoprazole, an MDR1 inhibitor. These findings indicate that the uptake and efflux transport activity of erythromycin affects its overall hepatic intrinsic clearance [65].

For the transporter substrates, detoxification in the liver consists of (1) hepatic uptake from the blood to hepatocytes (PS_{inf}), (2) backflux from hepatocytes to the blood (PS_{eff}), (3) biliary excretion from hepatocytes to bile (PS_{ex}), and (4) metabolism in hepatocytes (CL_{met}) (Fig. 13.8) [66]. In this case, the apparent overall hepatic intrinsic clearance ($CL_{int,all}$) can be described by the following equation.

$$CL_{int,all} = PS_{inf}\frac{PS_{ex} + CL_{met}}{PS_{eff} + PS_{ex} + CL_{met}} \tag{13.12}$$

If PS_{eff} is much lower than the sum of PS_{ex} and CL_{met}, according to Equation 13.12, the overall hepatic intrinsic clearance approximates the intrinsic uptake clearance (PS_{inf}).

$$CL_{int,all} \sim PS_{inf} \tag{13.13}$$

This equation means that the overall hepatic intrinsic clearance is solely dominated by the uptake activity of drugs, even if they are eliminated from the body mainly by metabolism. This situation is often called "uptake-limited clearance." On the other hand, if PS_{eff} is much greater than the sum of PS_{ex} and CL_{met}, the overall intrinsic clearance can be described as

$$CL_{int,all} = PS_{inf}\frac{PS_{ex} + CL_{met}}{PS_{eff}} \tag{13.14}$$

In this case, the intrinsic clearances of all the processes affect the overall hepatic intrinsic clearance. If drugs can rapidly penetrate the plasma membrane by passive diffusion, we can assume symmetrical membrane transport ($PS_{inf} = PS_{eff}$) and PS_{eff} is

much larger than $PS_{ex} + CL_{met}$. Under these assumptions, the overall hepatic intrinsic clearance described in Equation 13.12 can approximate the metabolic intrinsic clearance (CL_{met}).

$$CL_{int,all} \sim CL_{met} \tag{13.15}$$

It must be noted that the prediction of hepatic intrinsic clearance from *in vitro* metabolic clearance with liver microsomes or cytosol fractions can succeed only in limited situations, even if drugs are metabolized extensively in the liver.

We sometimes define "β value" according to the following equation.

$$\beta = \frac{PS_{ex} + CL_{met}}{PS_{eff} + PS_{ex} + CL_{met}} \tag{13.16}$$

On the basis of Equation 13.12, $CL_{int,all}$ can be described as

$$CL_{int,all} = PS_{inf} \times \beta \tag{13.17}$$

Thus, β is a kind of indicator representing whether the rate-limiting step of hepatic intrinsic clearance is likely to be an uptake process or not. The β value affects the change in the overall intrinsic clearance when each parameter is altered. Figure 13.9 shows the impact of the β value on the change in the overall intrinsic clearance when PS_{inf} or $CL_{met} + CL_{ex}$ are decreased. When the β value is close to 1, $CL_{int,all}$ approximates PS_{inf} as in Equation 13.13, and thus, a small decrease in the $CL_{met} + CL_{ex}$ value has little effect on the reduction of $CL_{int,all}$. On the other hand, when the β value is small, $CL_{int,all}$ becomes as described in Equation 13.14 and it becomes proportional to the $CL_{met} + CL_{ex}$ value. Therefore, the decrease in the $CL_{met} + CL_{ex}$ value affects the reduction of $CL_{int,all}$ directly. Conversely, a decrease in PS_{inf} value always affects $CL_{int,all}$ to the same degree regardless of the β value because $CL_{int,all}$ is proportional to PS_{inf} as shown in Equation 13.12. These simulation results tell us that the inhibition of influx transporters decreases $CL_{int,all}$ irrespective of the β value, while the inhibition of metabolic enzymes and/or biliary efflux transporters do not always have a direct

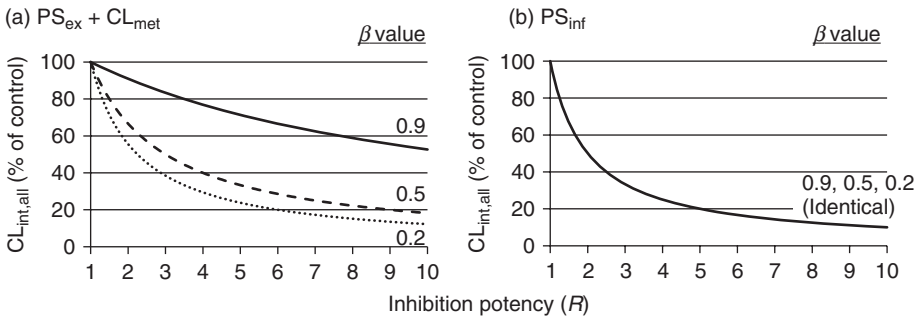

Figure 13.9 Impact of the β value on changes in the overall intrinsic clearance. Theoretical calculation of the change in the overall intrinsic clearance ($CL_{int,all}$) of a drug, whose β value is set at a designated value (0.9, 0.5, or 0.2) and is performed when $PS_{ex} + CL_{met}$ (a) or PS_{inf} (b) is specifically decreased to $1/R$.

effect on $CL_{int,all}$, if drugs are substrates of uptake transporters. We must also note that the intrinsic clearance of drugs with a β value of almost 1 can be decreased if CL_{met} or CL_{ex} are suppressed drastically and the β value itself becomes less than 1 after a change in CL_{met} or CL_{ex} (Fig. 13.9).

Watanabe *et al*. [67] have demonstrated that rat *in vivo* biliary and renal clearances with regard to the plasma concentration of several transporter substrate drugs were well predicted from *in vitro* uptake experiments using isolated rat hepatocytes and kidney slices, respectively, except for a few compounds whose renal clearance is very small, possibly because of the involvement of reabsorption. This concept was also successfully applied to human's case [68]. It has been also shown that the *in vivo* $CL_{int,all}$ values of four kinds of statins (pravastatin, pitavastatin, atorvastatin, and fluvastatin), two of which are eliminated from the body by extensive CYP-mediated metabolism, were similar to the uptake intrinsic clearance estimated using the multiple indicator dilution (MID) method in rats or in an uptake assay using cryopreserved human hepatocytes in humans. By contrast, the metabolic intrinsic clearance obtained from an *in vitro* metabolism assay with rat or human liver microsomes considerably underestimated the *in vivo* $CL_{int,all}$ value (Fig. 13.10) [69]. This evidence suggested that the rate-limiting step of hepatic intrinsic clearance of these statins is in the hepatic uptake process and that their β values are expected to be close to 1. Soars *et al*. also indicated that *in vitro* clearance estimated from the disappearance of compounds from the incubation media in an *in vitro* assay using hepatocytes ("media loss" assay) could explain their *in vivo*

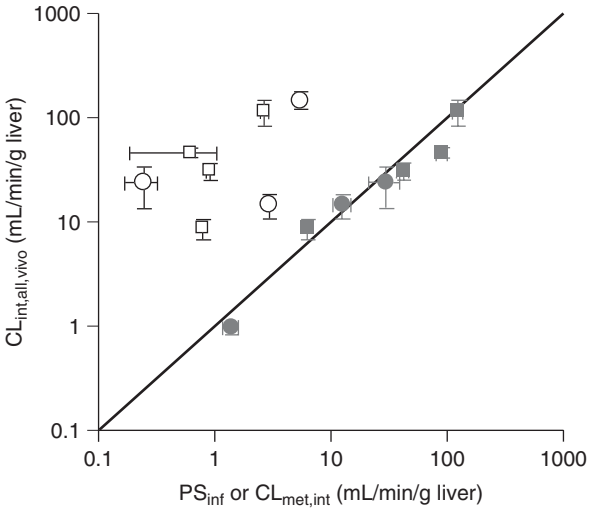

Figure 13.10 Rate-determining process of the hepatic intrinsic clearance of statins. The *in vivo* hepatic intrinsic clearances ($CL_{int,all,vivo}$) of four kinds of statins (pitavastatin, fluvastatin, atorvastatin, and pravastatin) in rats and humans are plotted against the uptake clearance or metabolic clearance. Closed circles, predicted from uptake clearance in human cryopreserved hepatocytes; open circles, predicted from metabolic clearance in human liver microsomes; closed squares, predicted from uptake clearance in rats determined using an MID (multiple indicator dilution) method; open squares, predicted from metabolic clearance in rat liver microsomes. The straight line indicates a 1:1 correlation. *Source*: This figure is cited from Ref. 69.

TABLE 13.2 Drugs That are Substrates of Both Metabolic Enzymes and Uptake Transporters

Substrates	Transporter	Metabolic Enzymes
Atorvastatin	OATPs	CYP3A4
Cerivastatin	OATPs	CYP2C8, 3A4
Fluvastatin	OATPs	CYP2C9
Repaglinide	OATPs	CYP2C8, 3A4
Nateglinide	OATPs	CYP2C9, 3A4
Glibenclamide	OATPs	CYP2C9, 3A4
Bosentan	OATPs	CYP2C9, 3A4
Torasemide	OATPs	CYP2C9
Gimatecan	OATPs	CYP3A4
Lopinavir	OATPs	CYP3A4
Docetaxel	OATP1B3	CYP3A4
Telmisartan	OATP1B3	UGTs

hepatic clearance better compared with the use of a conventional assay measuring the metabolite formation clearance with regard to the intracellular unbound concentration of compounds in the hepatocytes. This suggests the importance of uptake transporters in the determination of the overall intrinsic clearance in hepatocytes for some compounds [70,71].

The number of drugs that are substrates of both uptake transporters and are metabolic enzymes and eliminated from the body by extensive metabolism has been increasing gradually, as shown in Table 13.2. The pharmacokinetics of most of these OATP substrate drugs are altered by the coadministration of potent OATP inhibitors such as cyclosporine A and rifampicin and by genetic polymorphisms of OATP1B1 (e.g., T521C) [72,73]. For predicting changes in the pharmacokinetics of these drugs, their β values are essential, but they have not yet been estimated correctly.

Maeda *et al*. [74] have performed a clinical study in humans *in vivo* to demonstrate the rate-limiting step of the hepatic clearance of atorvastatin, a substrate of both OATP transporters and CYP3A4. In this study, a cocktail of a microdose of atorvastatin and of probe drugs for CYP3A4 (midazolam) and hepatic OATPs (pravastatin) was administered simultaneously to healthy volunteers. Changes in pharmacokinetics induced by the coadministration of a selective inhibitor for CYP3A4 [200 mg itraconazole (i.v.)] or for OATPs [600 mg rifampicin (single p.o.)] were observed. As expected, the plasma AUC of midazolam was increased only when it was coadministered with itraconazole, but not with rifampicin, whereas that of pravastatin was increased only by coadministration with rifampicin, but not with itraconazole. These results suggest the selective inhibition of CYP3A4 and OATPs by itraconazole and rifampicin, respectively. Under such conditions, the plasma AUC of atorvastatin was drastically increased by coadministration of rifampicin, but not itraconazole, although the plasma concentration of 2-hydroxy atorvastatin, one of the major metabolites of atorvastatin produced by CYP3A4, was decreased. This suggested that the hepatic clearance of atorvastatin is mainly dominated by hepatic uptake processes mediated by OATP transporters in humans.

13.2.3 Relationship Between Intrinsic Clearance and Organ Clearance

Organ clearance, defined as the rate of elimination of drugs divided by their blood concentration, is dominated not only by tissue intrinsic clearance but also by the blood flow rate in tissues and by the blood unbound fraction. Thus, a change in the tissue intrinsic clearance discussed above does not always lead to a change in organ clearance and subsequent alterations in the blood concentrations of drugs. To consider the effect of change in the intrinsic clearance on the pharmacokinetics of drugs, one of the important factors is the relative contribution of organ clearance to the total clearance (CL_{tot}). In general, drugs are eliminated mainly from the liver and kidney. Therefore, the total clearance can be described as in Equation 13.18.

$$CL_{tot} = CL_h + CL_r + CL_{others} \tag{13.18}$$

Here, CL_h, CL_r, and CL_{others}, respectively, represent the hepatic clearance, renal clearance, and clearance from other organs (if applicable). It is understood that the pharmacokinetics of a drug mainly eliminated from the kidney are changed little even if the hepatic clearance of the drug is largely decreased.

There are several models that relate the intrinsic organ clearance to organ clearance, such as the well-stirred model, the parallel tube model, and the dispersion model. The well-stirred model is used most frequently because of its simple mathematical handling. In this model, there is rapid and complete mixing, hence the term *well stirred*, of drugs coming from the blood circulation and blood in the tissue, and the blood concentration of drugs at the exit of tissue is assumed to be equal to that inside the tissue. In this condition, hepatic clearance (CL_h) can be expressed as in Equation 13.19.

$$CL_h = \frac{Q_h \cdot f_B \cdot CL_{int,h}}{Q_h + f_B \cdot CL_{int,h}} \tag{13.19}$$

Here, Q_h, f_B, and $CL_{int,h}$ represent the hepatic blood flow rate, blood unbound fraction of a drug, and the hepatic intrinsic clearance of a drug, respectively. For the kidney, we must consider the contribution of glomerular filtration, secretion, and reabsorption, and the renal clearance is described as

$$CL_r = \left(f_B \cdot GFR + \frac{Q_r \cdot f_B \cdot CL_{int,r}}{Q_r + f_B \cdot CL_{int,r}} \right) (1 - FR) \tag{13.20}$$

Here, GFR, Q_r, $CL_{int,r}$, and FR represent the glomerular filtration rate, renal blood flow rate, intrinsic renal secretion clearance, and fraction of drug reabsorbed from the urine, respectively.

Let us consider the relationship between intrinsic organ clearance and organ clearance by selecting two extreme cases. When Q_h is much smaller than $f_B CL_{int,h}$, Equation 13.19 is approximated by Equation 13.21.

$$CL_h \sim Q_h \tag{13.21}$$

Thus, hepatic clearance is only dominated by the hepatic blood flow rate, and a change in the hepatic intrinsic clearance does not alter the hepatic clearance

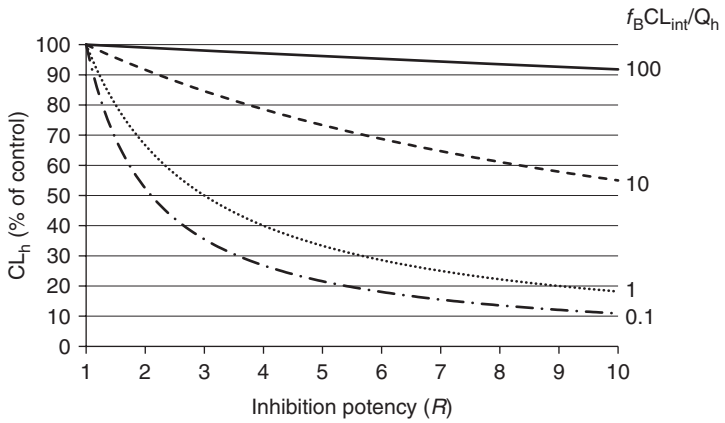

Figure 13.11 The impact of the ratio of $f_B CL_{int,h}$ to Q_h values on changes in the hepatic clearance (CL_h). This shows a theoretical calculation of changes in the CL_h of a drug, whose $f_B CL_{int,h}/Q_h$ value is set at a designated value (100, 10, 1, or 0.1) when $CL_{int,h}$ is decreased to $1/R$.

("blood-flow-limited clearance"). In contrast, when Q_h is much larger than $f_B CL_{int,h}$, Equation 13.19 is approximated by Equation 13.22.

$$CL_h \sim f_B CL_{int,h} \tag{13.22}$$

In this situation, hepatic clearance is proportional to the hepatic intrinsic clearance. Thus, the change in the hepatic intrinsic clearance should affect hepatic clearance directly ("intrinsic clearance-limited clearance"). Figure 13.11 shows the impact of the ratio of $f_B CL_{int,h}$ to Q_h on the change in the CL_h value when $CL_{int,h}$ is decreased. If $f_B CL_{int,h}$ is larger than Q_h, CL_h approximates Q_h (Eq. 13.21) and it is not changed so much when $CL_{int,h}$ is decreased. On the other hand, if $f_B CL_{int,h}$ is larger than Q_h, CL_h approximates $f_B CL_{int,h}$ (Eq. 13.22) and it is affected directly by a decrease in $CL_{int,h}$. When drugs are administered orally, if they are eliminated only from the liver, the blood AUC of drugs (AUC_{oral}) can be described by the following equation.

$$AUC_{oral} = \frac{F_a F_g \cdot F_h \cdot Dose}{CL_h} = \frac{F_a F_g \frac{Q_h}{Q_h + f_B CL_{int,h}} Dose}{\frac{Q_h \cdot f_B CL_{int,h}}{Q_h + f_B CL_{int,h}}} = \frac{F_a F_g \cdot Dose}{f_B CL_{int,h}} \tag{13.23}$$

Here, $F_a F_g$ and F_h represent intestinal availability and hepatic availability, respectively. From Equation 13.23, it should be noted that after the oral administration of drugs, their blood AUC is solely dominated by the hepatic intrinsic clearance, but not by the hepatic blood flow rate, regardless of the rate-limiting step of hepatic clearance.

13.3 PHYSIOLOGICALLY BASED PHARMACOKINETIC MODELING

As discussed above, organ clearance is regulated by multiple factors such as functions of various uptake/efflux transporters and metabolic enzymes. Because the overall

clearance in each organ cannot be described simply as the sum or product of the activity of each molecule, it is necessary to consider the detoxification machineries in each organ and in the body as a *system*. PBPK (physiologically based pharmacokinetic) modeling is one powerful tool that enables us to reconstruct detoxification systems in the body, based on the quantitative functions of multiple molecules and physiological parameters as a mathematical model. Rowland *et al*. [75] first described the clearance concept and a PBPK model for the liver in 1973. Then, as molecules dominating pharmacokinetics have been rapidly cloned and characterized, whole-body PBPK models for several drugs based on the accumulated knowledge of molecules have been constructed and analyzed by many pharmaceutical studies. In a PBPK model, the organs and circulating blood are expressed as compartments and movements of drugs from and to the compartment such as influx, efflux, and metabolism are represented as arrows, and these compartments are connected with the blood flow. Then, several physiological parameters such as organ volume and blood flow rate and drug-dependent parameters such as kinetic parameters for each enzyme and transporter are determined, and differential equations for individual compartments are formulated. Normally, in humans, we can only collect the blood and urine samples to quantify the drug concentration, and the number of sample collections should be limited. Moreover, it is almost impossible to measure the drug concentration in human tissues, which makes it difficult to predict the pharmacological/toxicological effects of drugs. In such situations, once we can construct an appropriate PBPK model, the time-dependent drug concentration in the plasma and all the tissues incorporated into the model can be simulated easily *in silico*. The US FDA clearly recommends the use of dynamic models for the accurate prediction of drug–drug interactions in the process of drug development in its recently published draft guidance about drug–drug interactions (http://www.fda.gov/downloads/Drugs/GuidanceComplianceRegulatoryInformation/Guidances/UCM292362.pdf). Recently, several FDA-based researchers have published papers showing the importance of PBPK modeling for the drug development. For example, Zhao *et al*. [76] described a number of examples for the use of PBPK models in efficient decision making during a regulatory review at the FDA, and Huang and Malcolm [77] discussed the use of simulation with PBPK modeling to address regulatory questions in clinical pharmacology reviews.

Figure 13.12 shows examples of organ models [78]. If membrane transport of drugs is mainly determined by passive diffusion, and rapid equilibrium of drugs between the blood and organ compartments can be assumed, a single compartment is enough to represent the tissue concentration of drugs as shown in Fig. 13.12(a). Assuming that drugs are well mixed inside a compartment, the blood concentration of drugs inside the tissue is thought to be equal to that at the exit of the compartment. Thus, the differential equations for tissue and the blood compartment can be described as

$$\text{Blood} : V_{\mathrm{B}} \frac{\mathrm{d}C_{\mathrm{B}}}{\mathrm{d}t} = -Q_{\mathrm{T}} \cdot C_{\mathrm{B}} + Q_{\mathrm{T}} \cdot \frac{C_{\mathrm{T}}}{K_{\mathrm{p}}} \tag{13.24}$$

$$\text{Tissue} : V_{\mathrm{T}} \frac{\mathrm{d}C_{\mathrm{T}}}{\mathrm{d}t} = Q_{\mathrm{T}} \cdot C_{\mathrm{B}} - Q_{\mathrm{T}} \frac{C_{\mathrm{T}}}{K_{\mathrm{p}}} - f_{\mathrm{B}} \mathrm{CL}_{\mathrm{int}} \frac{C_{\mathrm{T}}}{K_{\mathrm{p}}} \tag{13.25}$$

Here, V_{T} is the tissue volume, C_{T} the drug concentration in the tissue, C_{B} the drug concentration in the blood, Q_{T} the blood flow rate in the tissue, K_{p} the tissue-to-plasma

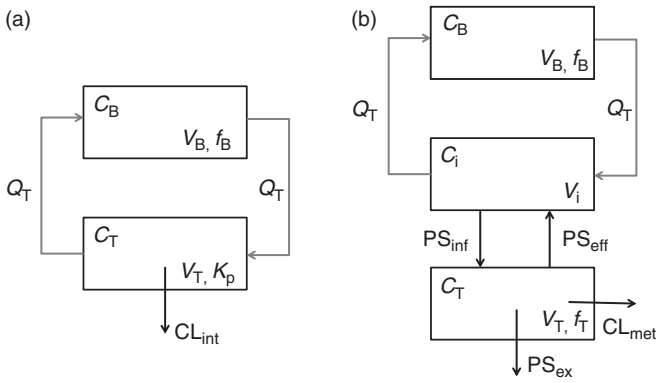

Figure 13.12 Examples of simple models expressing the detoxification ability of organs. (a) Model for drugs whose membrane transport is mainly determined by passive diffusion and where rapid equilibrium between blood and organ can be assumed. (b) Model for drugs that are taken up into organs by active transporters.

concentration ratio, f_B the protein unbound fraction in the blood, and CL_{int} the tissue intrinsic clearance.

On the other hand, if active transport is involved in the membrane permeation of drugs, the inlet and tissue compartments should be separated to represent the membrane transport clearance as shown in Fig. 13.12(b). In this case, the differential equations for blood, inlet, and tissue concentrations are described as in Equations 13.26–13.28.

$$\text{Blood} : V_B \frac{dC_B}{dt} = -Q_T \cdot C_B + Q_T \cdot C_i \tag{13.26}$$

$$\text{Inlet} : V_i \frac{dC_i}{dt} = Q_T \cdot C_B - Q_T \cdot C_i - f_B PS_{inf} \cdot C_i + f_T PS_{eff} \cdot C_T \tag{13.27}$$

$$\text{Tissue} : V_T \frac{dC_T}{dt} = f_B PS_{inf} \cdot C_i - (PS_{eff} + PS_{ex} + CL_{met}) f_T C_T \tag{13.28}$$

Here, V_i is the inlet volume, C_i the drug concentration in the inlet compartment, and f_T the protein unbound fraction in the tissue.

By integrating these equations, the blood and tissue AUCs of drugs are represented as follows [79].

$$AUC_B = \frac{\text{Dose}}{f_B \cdot PS_{inf} \frac{PS_{ex} + CL_{met}}{PS_{eff} + PS_{ex} + CL_{met}}} = \left(\frac{\text{Dose}}{f_B \cdot CL_{int,all}} \right) \tag{13.29}$$

$$AUC_T = \frac{\text{Dose}}{f_T (PS_{ex} + CL_{met})} \tag{13.30}$$

These equations demonstrate important messages about the different changes in blood and tissue concentrations when each intrinsic clearance is altered. As mentioned

in Section 13.2.2, if $PS_{ex} + CL_{met}$ is much larger than PS_{eff}, Equation 13.29 approximates Dose/$f_B PS_{inf}$. Under this condition, when the hepatic uptake activity (PS_{inf}) is decreased, the blood AUC is increased, while the tissue AUC is not changed. Conversely, when the intrinsic clearance of biliary excretion (PS_{ex}) and/or metabolism (CL_{met}) are decreased, the blood AUC is unchanged, whereas the tissue AUC is increased inversely with ($PS_{ex} + CL_{met}$).

Watanabe *et al*. [79] have constructed a PBPK model of pravastatin, which is a substrate of OATPs and MRP2 in the liver (Fig. 13.13(a)). In this model, the liver compartment was divided into five compartments to mimic the dispersion model because the hepatic clearance of pravastatin is very close to the hepatic blood flow rate. The same intrinsic clearance of hepatic influx, backflux, biliary excretion, and metabolic clearance were set up in each segment. Then, all the kinetic parameters were set up only from the results of *in vitro* experiments using a simple scaling-up method. The intrinsic clearances of influx and passive diffusion of pravastatin were determined from uptake studies using isolated hepatocytes, intrinsic clearance of biliary excretion was determined from ATP-dependent transport using canalicular membrane vesicles (CMVs), and metabolic intrinsic clearance was determined from a metabolism assay using the liver S9 fraction. They confirmed the time profiles of the plasma concentration and cumulative biliary excreted amount of pravastatin at several doses in rats and the plasma concentrations after intravenous and oral administration of pravastatin in humans were well reproduced by simulation in this PBPK model. One of the advantages of a PBPK model is in performing sensitivity analysis. This is a good method to identify critical processes dominating the phenotype (e.g., plasma and tissue concentrations) by monitoring any alteration of the target phenotype when specific process is changed *in silico*. Watanabe *et al*. performed the same type of simulation to understand the effects of changes in each intrinsic clearance on the plasma and hepatic concentrations of pravastatin. As shown in Fig. 13.13(b), changes in the influx intrinsic clearance largely altered the plasma concentration but not the hepatic concentration. However, changes in the biliary excretion intrinsic clearance greatly altered the hepatic concentration but not the plasma concentration, which is very similar to the results obtained from the simple model discussed above (Fig. 13.12(b)). A PBPK model also enables us to simulate the severity of drug–drug interactions accurately by connecting the PBPK models of substrate drugs and inhibitors to their target enzymes/transporters. For example, Kanamitsu *et al*. [80] predicted a lethal drug–drug interaction between 5-FU and sorivudine by connecting the PBPK models of 5-FU, sorivudine, and its metabolite, (E)-5-(2-bromovinyl) uracil (BVU). This drug–drug interaction is caused by the mechanism-based inactivation of dihydropyrimidine dehydrogenase (DPD), which is a major metabolizing enzyme of 5-FU, by BVU. As a result, they succeeded in reproducing a great decrease in the hepatic content of active DPD and a subsequent dramatic increase in the plasma concentration of 5-FU by coadministration of sorivudine in an *in silico* simulation. As a whole, by utilizing a PBPK model, we can simulate the plasma and tissue concentrations of drugs in any virtual situation easily by changing the parameters in the model without any additional clinical studies. This greatly helps pharmaceutical researchers to optimize the pharmacokinetic properties of drugs because it is very difficult to estimate the target outcome intuitively from the complicated whole-body drug detoxification system.

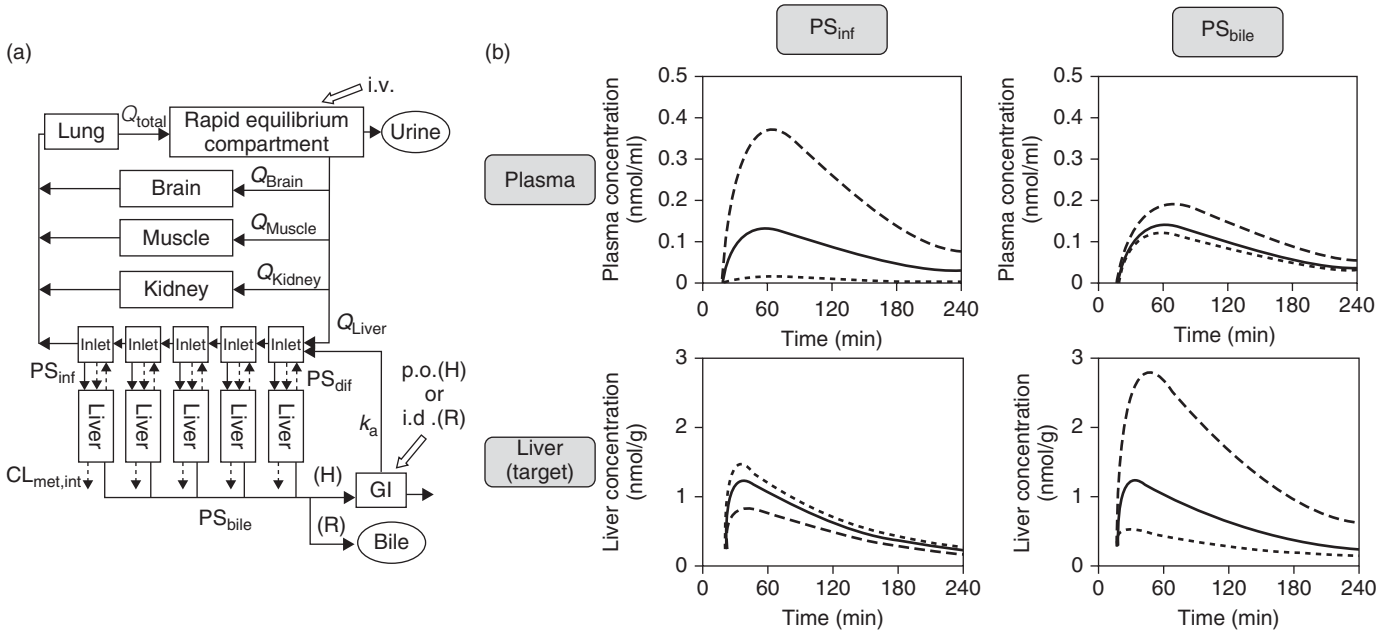

Figure 13.13 Simulation of plasma and liver concentration of pravastatin by using a PBPK (physiologically based pharmacokinetic) model. (a) Structure of PBPK model for pravastatin. (b) Simulated time profiles of plasma and liver concentrations of pravastatin when PS_{inf} or PS_{bile} values are increased threefold (broken line) or decreased by one-third (dotted line) compared with the control value (solid line). *Source*: This figure is cited from Ref. 79.

13.4 CONCLUSION

In this chapter, we have overviewed the combinations of molecules responsible for the detoxification of drugs in the liver and kidney and have discussed the quantitative importance of each intrinsic process in the overall performance of detoxification systems from a pharmacokinetic viewpoint. We have also discussed the significant role of the PBPK model for the better understanding of complex systems and quantitatively predicting target outcomes in the process of drug development. Major molecules involved in the detoxification of drugs have already been identified and characterized by *in vitro* assay systems. Thus, we can construct a PBPK model simply by integrating the kinetic parameters of all the molecular-based processes without any empirical parameters. However, the general procedures to set up parameters in any PBPK model from *in vitro* data must be investigated further and validated. Because molecular mechanisms and their networks of pharmacodynamic (PD) processes are very complicated and still not fully understood for most drugs, molecular-based PD models have not been used often, although the concept of mechanistic PK/PD modeling has been established. To construct the correct PD model, it is necessary to have a wide variety of real data sets in different conditions for a thorough validation of the entire complex model because so many parameters dominate the model. Systems biological approaches such as proteomics and metabolomics might help overcome this issue. During the drug discovery and development process, such models representing the molecular systems of detoxification and pharmacological actions of drugs greatly save time and human resources by skipping unnecessary clinical studies. They enable us to predict the pharmacokinetics of drugs in special situations such as with genetic polymorphisms of molecules, drug–drug interactions, and pathophysiological conditions without using any clinical studies. Therefore, general procedures of the construction, data acquisition, and validation of models need to be established.

REFERENCES

1. Giacomini KM, Sugiyama Y. Membrane transporters and drug response. In: Brunton LL, Cahbner BA, Knollmann BC, editors. Goodman and Gilman's the pharmacological basis of therapeutics. 12th ed. New York: McGraw-Hill; 2011. pp. 89–121.
2. Adson A, Raub TJ, Burton PS, *et al*. Quantitative approaches to delineate paracellular diffusion in cultured epithelial cell monolayers. J Pharm Sci 1994; 83:1529–1536.
3. Yamazaki M, Akiyama S, Ni'inuma K, *et al*. Biliary excretion of pravastatin in rats: contribution of the excretion pathway mediated by canalicular multispecific organic anion transporter. Drug Metab Dispos 1997;25:1123–1129.
4. Shitara Y, Sugiyama Y. Pharmacokinetic and pharmacodynamic alterations of 3-hydroxy-3-methylglutaryl coenzyme A (HMG-CoA) reductase inhibitors: drug-drug interactions and interindividual differences in transporter and metabolic enzyme functions. Pharmacol Ther 2006;112:71–105.
5. Fahrmayr C, Fromm MF, Konig J. Hepatic OATP and OCT uptake transporters: their role for drug-drug interactions and pharmacogenetic aspects. Drug Metab Rev 2010;42:380–401.
6. Terada T, Inui K. Physiological and pharmacokinetic roles of H^+/organic cation antiporters (MATE/SLC47A). Biochem Pharmacol 2008;75:1689–1696.

7. Kusuhara H, Sugiyama Y. Vectorial Transport II. In: Kusuhara H, Sugiyama Y, editors. Molecular Pharmacokinetics. Tokyo: Nanzando; 2008. pp. 364–376. (written in Japanese).
8. Dawson PA, Lan T, Rao A. Bile acid transporters. J Lipid Res 2009;50:2340–2357.
9. Maeda K, Sugiyama Y. *In vitro-in vivo* scale-up of drug transport activities. In: You G, Morris ME, editors. Drug transporters. New Jersey: John Wiley and Sons, Inc.; 2007. pp. 557–588.
10. Yamashiro W, Maeda K, Hirouchi M, *et al*. Involvement of transporters in the hepatic uptake and biliary excretion of valsartan, a selective antagonist of the angiotensin II AT1-receptor, in humans. Drug Metab Dispos 2006;34:1247–1254.
11. Ishiguro N, Maeda K, Kishimoto W, *et al*. Predominant contribution of OATP1B3 to the hepatic uptake of telmisartan, an angiotensin II receptor antagonist, in humans. Drug Metab Dispos 2006;34:1109–1115.
12. Rizwan AN, Burckhardt G. Organic anion transporters of the SLC22 family: biopharmaceutical, physiological, and pathological roles. Pharm Res 2007;24:450–470.
13. Koepsell H, Lips K, Volk C. Polyspecific organic cation transporters: structure, function, physiological roles, and biopharmaceutical implications. Pharm Res 2007;24:1227–1251.
14. Maeda K, Suzuki H, Sugiyama Y. Hepatic transport. In: van De Waterbeemd H, Testa B, editors. Drug bioavailability. Weinheim: Wiley-VCH; 2009. pp. 277–332.
15. Ito S, Kusuhara H, Kuroiwa Y, *et al*. Potent and specific inhibition of mMate1-mediated efflux of type I organic cations in the liver and kidney by pyrimethamine. J Pharmacol Exp Ther 2010;333:341–350.
16. Tsuda M, Terada T, Mizuno T, *et al*. Targeted disruption of the multidrug and toxin extrusion 1 (mate1) gene in mice reduces renal secretion of metformin. Mol Pharmacol 2009;75:1280–1286.
17. Cui Y, Konig J, Keppler D. Vectorial transport by double-transfected cells expressing the human uptake transporter SLC21A8 and the apical export pump ABCC2. Mol Pharmacol 2001;60:934–943.
18. Sasaki M, Suzuki H, Ito K, *et al*. Transcellular transport of organic anions across a double-transfected Madin-Darby canine kidney II cell monolayer expressing both human organic anion-transporting polypeptide (OATP2/SLC21A6) and Multidrug resistance-associated protein 2 (MRP2/ABCC2). J Biol Chem 2002;277:6497–6503.
19. Sasaki M, Suzuki H, Aoki J, *et al*. Prediction of *in vivo* biliary clearance from the *in vitro* transcellular transport of organic anions across a double-transfected Madin-Darby canine kidney II monolayer expressing both rat organic anion transporting polypeptide 4 and multidrug resistance associated protein 2. Mol Pharmacol 2004;66:450–459.
20. Matsushima S, Maeda K, Kondo C, *et al*. Identification of the hepatic efflux transporters of organic anions using double-transfected Madin-Darby canine kidney II cells expressing human organic anion-transporting polypeptide 1B1 (OATP1B1)/multidrug resistance-associated protein 2, OATP1B1/multidrug resistance 1, and OATP1B1/breast cancer resistance protein. J Pharmacol Exp Ther 2005;314:1059–1067.
21. Morikawa A, Goto Y, Suzuki H, *et al*. Biliary excretion of 17beta-estradiol 17beta-D-glucuronide is predominantly mediated by cMOAT/MRP2. Pharm Res 2000;17:546–552.
22. Yamazaki M, Kobayashi K, Sugiyama Y. Primary active transport of pravastatin across the liver canalicular membrane in normal and mutant Eisai hyperbilirubinemic rats. Biopharm Drug Dispos 1996;17:607–621.
23. Kopplow K, Letschert K, Konig J, *et al*. Human hepatobiliary transport of organic anions analyzed by quadruple-transfected cells. Mol Pharmacol 2005;68:1031–1038.
24. Nies AT, Herrmann E, Brom M, *et al*. Vectorial transport of the plant alkaloid berberine by double-transfected cells expressing the human organic cation transporter 1 (OCT1, SLC22A1) and the efflux pump MDR1 P-glycoprotein (ABCB1). Naunyn Schmiedebergs Arch Pharmacol 2008;376:449–461.

25. Konig J, Zolk O, Singer K, *et al*. Double-transfected MDCK cells expressing human OCT1/MATE1 or OCT2/MATE1: determinants of uptake and transcellular translocation of organic cations. Br J Pharmacol 2011;163:546–555.
26. Sato T, Masuda S, Yonezawa A, *et al*. Transcellular transport of organic cations in double-transfected MDCK cells expressing human organic cation transporters hOCT1/hMATE1 and hOCT2/hMATE1. Biochem Pharmacol 2008;76:894–903.
27. Masereeuw R, Russel FG. Therapeutic implications of renal anionic drug transporters. Pharmacol Ther 2010;126:200–216.
28. Mizuno N, Suzuki M, Kusuhara H, *et al*. Impaired renal excretion of 6-hydroxy-5,7-dimethyl-2-methylamino-4-(3-pyridylmethyl) benzothiazole (E3040) sulfate in breast cancer resistance protein (BCRP1/ABCG2) knockout mice. Drug Metab Dispos 2004;32:898–901.
29. Mizuno N, Takahashi T, Kusuhara H, *et al*. Evaluation of the role of breast cancer resistance protein (BCRP/ABCG2) and multidrug resistance-associated protein 4 (MRP4/ABCC4) in the urinary excretion of sulfate and glucuronide metabolites of edaravone (MCI-186; 3-methyl-1-phenyl-2-pyrazolin-5-one). Drug Metab Dispos 2007;35:2045–2052.
30. Imaoka T, Kusuhara H, Adachi-Akahane S, *et al*. The renal-specific transporter mediates facilitative transport of organic anions at the brush border membrane of mouse renal tubules. J Am Soc Nephrol 2004;15:2012–2022.
31. Anzai N, Jutabha P, Amonpatumrat-Takahashi S, *et al*. Recent advances in renal urate transport: characterization of candidate transporters indicated by genome-wide association studies. Clin Exp Nephrol 2011;16:89–95.
32. Jutabha P, Anzai N, Kitamura K, *et al*. Human sodium phosphate transporter 4 (hNPT4/SLC17A3) as a common renal secretory pathway for drugs and urate. J Biol Chem 2010;285:35123–35132.
33. Uchino H, Tamai I, Yamashita K, *et al*. p-aminohippuric acid transport at renal apical membrane mediated by human inorganic phosphate transporter NPT1. Biochem Biophys Res Commun 2000;270:254–259.
34. Fujita T, Urban TJ, Leabman MK, *et al*. Transport of drugs in the kidney by the human organic cation transporter, OCT2 and its genetic variants. J Pharm Sci 2006;95:25–36.
35. Ohashi R, Tamai I, Yabuuchi H, *et al*. Na(+)-dependent carnitine transport by organic cation transporter (OCTN2): its pharmacological and toxicological relevance. J Pharmacol Exp Ther 1999;291:778–784.
36. Damme K, Nies AT, Schaeffeler E, *et al*. Mammalian MATE (SLC47A) transport proteins: impact on efflux of endogenous substrates and xenobiotics. Drug Metab Rev 2011;43:499–523.
37. Yonezawa A, Inui K. Importance of the multidrug and toxin extrusion MATE/SLC47A family to pharmacokinetics, pharmacodynamics/toxicodynamics and pharmacogenomics. Br J Pharmacol 2011;164:1817–1825.
38. Kusuhara H, Ito S, Kumagai Y, *et al*. Effects of a MATE protein inhibitor, pyrimethamine, on the renal elimination of metformin at oral microdose and at therapeutic dose in healthy subjects. Clin Pharmacol Ther 2011;89:837–844.
39. Kamal MA, Jiang H, Hu Y, *et al*. Influence of genetic knockout of Pept2 on the *in vivo* disposition of endogenous and exogenous carnosine in wild-type and Pept2 null mice. Am J Physiol Regul Integr Comp Physiol 2009;296:R986–R991.
40. Gotoh Y, Kato Y, Stieger B, *et al*. Gender difference in the Oatp1-mediated tubular reabsorption of estradiol 17beta-D-glucuronide in rats. Am J Physiol Endocrinol Metab 2002;282:E1245–E1254.
41. Kato Y, Kuge K, Kusuhara H, *et al*. Gender difference in the urinary excretion of organic anions in rats. J Pharmacol Exp Ther 2002;302:483–489.
42. Niemi M, Backman JT, Neuvonen M, *et al*. Effects of gemfibrozil, itraconazole, and their combination on the pharmacokinetics and pharmacodynamics of repaglinide: potentially hazardous interaction between gemfibrozil and repaglinide. Diabetologia 2003;46:347–351.

43. Kusuhara H, Sugiyama Y. *In vitro-in vivo* extrapolation of transporter-mediated clearance in the liver and kidney. Drug Metab Pharmacokinet 2009;24:37–52.
44. Chen Y, Agarwal S, Shaik NM, *et al*. P-glycoprotein and breast cancer resistance protein influence brain distribution of dasatinib. J Pharmacol Exp Ther 2009;330: 956–963.
45. Lagas JS, van Waterschoot RA, van Tilburg VA, *et al*. Brain accumulation of dasatinib is restricted by P-glycoprotein (ABCB1) and breast cancer resistance protein (ABCG2) and can be enhanced by elacridar treatment. Clin Cancer Res 2009;15:2344–2351.
46. Oostendorp RL, Buckle T, Beijnen JH, *et al*. The effect of P-gp (Mdr1a/1b), BCRP (Bcrp1) and P-gp/BCRP inhibitors on the *in vivo* absorption, distribution, metabolism and excretion of imatinib. Invest New Drugs 2009;27:31–40.
47. Kodaira H, Kusuhara H, Ushiki J, *et al*. Kinetic analysis of the cooperation of P-glycoprotein (P-gp/Abcb1) and breast cancer resistance protein (Bcrp/Abcg2) in limiting the brain and testis penetration of erlotinib, flavopiridol, and mitoxantrone. J Pharmacol Exp Ther 2010;333:788–796.
48. Crespi CL, Penman BW. Use of cDNA-expressed human cytochrome P450 enzymes to study potential drug-drug interactions. Adv Pharmacol 1997;43:171–188.
49. Kouzuki H, Suzuki H, Ito K, *et al*. Contribution of sodium taurocholate co-transporting polypeptide to the uptake of its possible substrates into rat hepatocytes. J Pharmacol Exp Ther 1998;286:1043–1050.
50. Kouzuki H, Suzuki H, Ito K, *et al*. Contribution of organic anion transporting polypeptide to uptake of its possible substrates into rat hepatocytes. J Pharmacol Exp Ther 1999;288:627–634.
51. Hirano M, Maeda K, Shitara Y, *et al*. Contribution of OATP2 (OATP1B1) and OATP8 (OATP1B3) to the hepatic uptake of pitavastatin in humans. J Pharmacol Exp Ther 2004;311:139–146.
52. Ieiri I, Higuchi S, Sugiyama Y. Genetic polymorphisms of uptake (OATP1B1, 1B3) and efflux (MRP2, BCRP) transporters: implications for inter-individual differences in the pharmacokinetics and pharmacodynamics of statins and other clinically relevant drugs. Expert Opin Drug Metab Toxicol 2009;5:703–729.
53. Yamada A, Maeda K, Ishiguro N, *et al*. The impact of pharmacogenetics of metabolic enzymes and transporters on the pharmacokinetics of telmisartan in healthy volunteers. Pharmacogenet Genom 2011;21:523–530.
54. Hasegawa M, Kusuhara H, Endou H, *et al*. Contribution of organic anion transporters to the renal uptake of anionic compounds and nucleoside derivatives in rat. J Pharmacol Exp Ther 2003;305:1087–1097.
55. Hasegawa M, Kusuhara H, Sugiyama D, *et al*. Functional involvement of rat organic anion transporter 3 (rOat3; Slc22a8) in the renal uptake of organic anions. J Pharmacol Exp Ther 2002;300:746–753.
56. Deguchi T, Kusuhara H, Takadate A, *et al*. Characterization of uremic toxin transport by organic anion transporters in the kidney. Kidney Int 2004;65:162–174.
57. LeCluyse EL, Audus KL, Hochman JH. Formation of extensive canalicular networks by rat hepatocytes cultured in collagen-sandwich configuration. Am J Physiol 1994;266: C1764–C1774.
58. Liu X, LeCluyse EL, Brouwer KR, *et al*. Use of Ca2+ modulation to evaluate biliary excretion in sandwich-cultured rat hepatocytes. J Pharmacol Exp Ther 1999;289: 1592–1599.
59. Tian X, Zamek-Gliszczynski MJ, Zhang P, *et al*. Modulation of multidrug resistance-associated protein 2 (Mrp2) and Mrp3 expression and function with small interfering RNA in sandwich-cultured rat hepatocytes. Mol Pharmacol 2004;66:1004–1010.
60. Yue W, Abe K, Brouwer KL. Knocking down breast cancer resistance protein (Bcrp) by adenoviral vector-mediated RNA interference (RNAi) in sandwich-cultured rat hepatocytes:

a novel tool to assess the contribution of Bcrp to drug biliary excretion. Mol Pharm 2009;6:134–143.
61. Swift B, Yue W, Brouwer KL. Evaluation of (99 m)technetium-mebrofenin and (99 m)technetium-sestamibi as specific probes for hepatic transport protein function in rat and human hepatocytes. Pharm Res 2010;27:1987–1998.
62. Han YH, Kato Y, Sugiyama Y. Binding and transport of methotrexate and its derivative, MX-68, across the brush-border membrane in rat kidney. Biopharm Drug Dispos 1999;20:361–367.
63. Koren G, Klein J, Bentur Y, *et al*. The effects of mannitol diuresis on digoxin and phenobarbital handling by the kidney: implications for tubular reabsorption and secretion of the cardiac glycoside. Clin Invest Med 1989;12:279–284.
64. Lam JL, Benet LZ. Hepatic microsome studies are insufficient to characterize *in vivo* hepatic metabolic clearance and metabolic drug-drug interactions: studies of digoxin metabolism in primary rat hepatocytes versus microsomes. Drug Metab Dispos 2004;32:1311–1316.
65. Frassetto LA, Poon S, Tsourounis C, *et al*. Effects of uptake and efflux transporter inhibition on erythromycin breath test results. Clin Pharmacol Ther 2007;81:828–832.
66. Shitara Y, Horie T, Sugiyama Y. Transporters as a determinant of drug clearance and tissue distribution. Eur J Pharm Sci 2006;27:425–446.
67. Watanabe T, Maeda K, Kondo T, *et al*. Prediction of the hepatic and renal clearance of transporter substrates in rats using *in vitro* uptake experiments. Drug Metab Dispos 2009;37:1471–1479.
68. Watanabe T, Kusuhara H, Watanabe T, *et al*. Prediction of the overall renal tubular secretion and hepatic clearance of anionic drugs and a renal drug-drug interaction involving organic anion transporter 3 in humans by *in vitro* uptake experiments. Drug Metab Dispos 2011;39:1031–1038.
69. Watanabe T, Kusuhara H, Maeda K, *et al*. Investigation of the rate-determining process in the hepatic elimination of HMG-CoA reductase inhibitors in rats and humans. Drug Metab Dispos 2010;38:215–222.
70. Soars MG, Grime K, Sproston JL, *et al*. Use of hepatocytes to assess the contribution of hepatic uptake to clearance *in vivo*. Drug Metab Dispos 2007;35:859–865.
71. Soars MG, Webborn PJ, Riley RJ. Impact of hepatic uptake transporters on pharmacokinetics and drug-drug interactions: use of assays and models for decision making in the pharmaceutical industry. Mol Pharm 2009;6:1662–1677.
72. Nakanishi T, Tamai I. Genetic polymorphisms of OATP transporters and their impact on intestinal absorption and hepatic disposition of drugs. Drug Metab Pharmacokinet 2012;27:106–121.
73. Yoshida K, Maeda K, Sugiyama Y. Prediction of the degree of transporter-mediated drug-drug interactions involving OATP substrates based on *in vitro* inhibition studies. Clin Pharmacol Ther 2012. DOI: 10.1038/clpt.2011.351.
74. Maeda K, Ikeda Y, Fujita T, *et al*. Identification of the rate-determining process in the hepatic clearance of atorvastatin in a clinical cassette microdosing study. Clin Pharmacol Ther 2011;90:575–581.
75. Rowland M, Benet LZ, Graham GG. Clearance concepts in pharmacokinetics. J Pharmacokinet Biopharm 1973;1:123–136.
76. Zhao P, Zhang L, Grillo JA, *et al*. Applications of physiologically based pharmacokinetic (PBPK) modeling and simulation during regulatory review. Clin Pharmacol Ther 2011;89:259–267.
77. Huang SM, Rowland M. The role of physiologically based pharmacokinetic modeling in regulatory review. Clin Pharmacol Ther 2012;91:542–549.
78. Fan J, Chen S, Chow EC, *et al*. PBPK modeling of intestinal and liver enzymes and transporters in drug absorption and sequential metabolism. Curr Drug Metab 2010;11:743–761.

79. Watanabe T, Kusuhara H, Maeda K, *et al*. Physiologically based pharmacokinetic modeling to predict transporter-mediated clearance and distribution of pravastatin in humans. J Pharmacol Exp Ther 2009;328:652–662.
80. Kanamitsu SI, Ito K, Okuda H, *et al*. Prediction of *in vivo* drug-drug interactions based on mechanism-based inhibition from *in vitro* data: inhibition of 5-fluorouracil metabolism by (E)-5-(2-Bromovinyl)uracil. Drug Metab Dispos 2000;28:467–474.